INPUT SIGNAL GENERATION FOR BARRIER BUCKET RF SYSTEMS AT GSI*

J. Harzheim†, D. Domont-Yankulova, K. Groß, H. Klingbeil[1] TU Darmstadt, Darmstadt, Germany
M. Frey, GSI, Darmstadt, Germany
[1] also at GSI, Darmstadt, Germany

Abstract

At GSI, Barrier Bucket RF systems are currently designed for the SIS 100 synchrotron (part of the future accelerator facility FAIR) [1] and the Experimental Storage Ring (ESR) [2]. The purpose of these systems is to provide pulsed voltages (Fig. 1) at the cavity gap in order to facilitate several longitudinal bunch manipulations. To achieve the desired signal quality, the design and matching of the different components as well as a proper mathematical modeling of the system is needed. This contribution focuses on the system identification and modeling for the ESR Barrier Bucket system to calculate the input signal for the requested output voltage. In a first step, the system is modeled using a linear model, which is sufficient up to gap voltages of 550 V. At higher amplitudes, nonlinear effects begin to occur, reducing the output signal quality. Therefore, the linear model is extended to a Hammerstein model which consists of a static nonlinearity followed by the linear part. Measurement results show that this approach significantly improves the signal quality at high amplitudes.

INTRODUCTION

Barrier Bucket (BB) systems enable a large variety of longitudinal beam manipulations in synchrotrons and storage rings (e.g. [3-5]) by using pulsed gap voltages (see Fig. 1). If the repetition frequency of the voltage pulse equals the revolution frequency of the beam, this voltage pulse forms a stationary potential barrier in phase space. When both frequencies differ, the barrier is moving in phase space ("moving barriers", e.g. [6-8]). Particles moving in the ring can be confined between two barriers, allowing variable bucket lengths and applications like bunch merging, compression or decompression.

In order to deliver high intensity beams of high quality, as needed for the planned experiments at FAIR, requirements on the gap voltage qualities for acceleration and Barrier Bucket operation are very high as well. Hence, a lot of effort needs to be spent on the design of the system, but also on the proper mathematical modeling in order to be able to calculate the accurate input signal. At GSI, a prototype setup of the future ESR BB system is currently under investigation [9-10]. The three main components are a broadband cavity filled with Magnetic Alloy ring cores [11-13], a solid state amplifier (amplifier research 1000A225) and a signal generator (Keysight 3600A series 2-channel AWG). A simplified setup of the system is shown in Fig. 2.

* Work supported by BMBF and GSI
† harzheim@temf.tu-darmstadt.de

SIGNAL REQUIREMENTS

For the ESR BB system, single-sine voltage pulses with a repetition frequency f_{rep} of 900 kHz and a BB frequency f_{BB} of 5 MHz are required (see Fig. 1). The desired amplitude $\hat{U}_{BB}$ of the pulse is 1 kV. As voltages aside the pulse (so called "ringing") can lead to microbunching, the ringing must stay in ±2,5% of $\hat{U}_{BB}$. Additionally, the difference between positive and negative half cycle should be in the range of ±5% of $\hat{U}_{BB}$. The values were taken from [14].

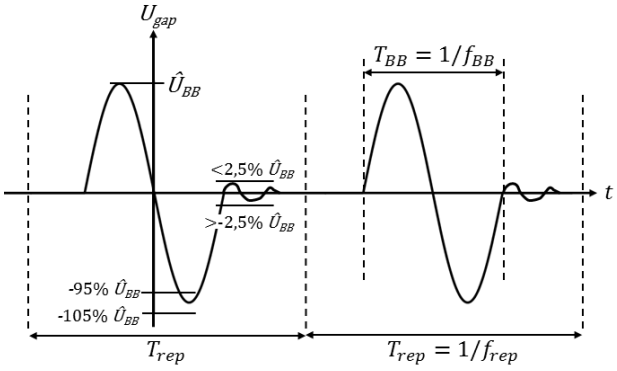

Figure 1: Desired output gap voltage.

LINEAR REGION

For sufficiently small input signals, most systems can be described by a linearization around the system's operating point. In this linear region, the relation between the input signal $\underline{U}_{AWG}(\omega) = \underline{U}_{in}(\omega)$ and the output signal $\underline{U}_{out}(\omega)$ is given by the system's frequency response $\underline{H}(\omega)$:

$$\underline{U}_{out}(\omega) = \underline{U}_{in}(\omega) \cdot \underline{H}(\omega). \quad (1)$$

For the prototype setup, the input signal is the signal created by the signal generator and the output signal is the voltage measured at the cavity gap.

In order to determine the input signal of the system, the frequency response has to be measured. For the measurement, a small signal frequency sweep from 10 kHz to 80 MHz was applied to the system. The sweep was performed sufficiently slowly (e.g. 25 minutes) to ensure steady state conditions.

A two channel AWG was used as a signal generator with channel 1 connected to the RF power amplifier and channel 2 connected to the oscilloscope to measure the undistorted input signal $\underline{U}_{in}$. The output signal $\underline{U}_{out}$ (voltage at the cavity gap) was measured using the same oscilloscope.

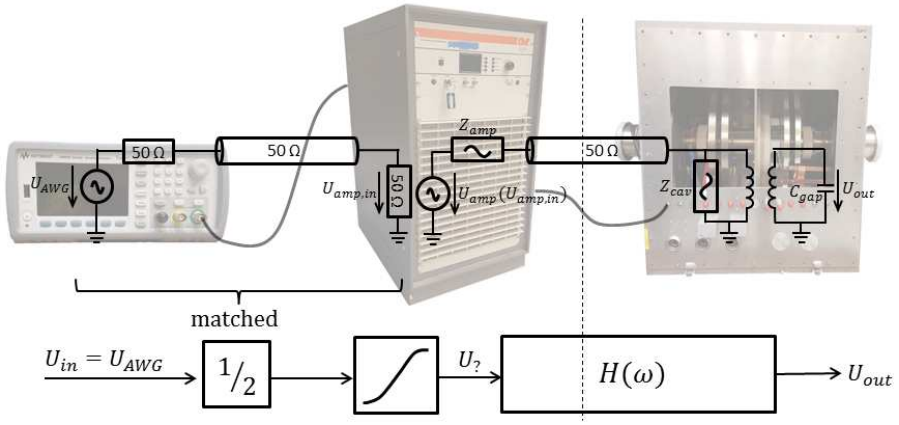

Figure 2: Hammerstein modeling of the ESR BB prototype system.

This way, the difference in amplitude and phase between input and output signal can be observed at each frequency point. $\underline{H}(\omega)$ can be calculated from measurement data by

$$\underline{H}(\omega) = \frac{\underline{U}_{out}(\omega)}{\underline{U}_{in}(\omega)}. \tag{2}$$

The measured amplitude response of the system is shown in Fig. 3.

For periodic BB operation (see Fig. 1), the desired output signal during one period T_{rep} is defined as

$$U_{out}(t) = \begin{cases} -\hat{U} \cdot \sin\left(\frac{2\pi}{T_{BB}} t\right) & \text{for} \quad -\frac{T_{BB}}{2} < t < \frac{T_{BB}}{2} \\ 0 & \text{else} \end{cases}. \tag{3}$$

Using Fourier decomposition [15], the signal can be described by

$$U_{out}(t) = \sum_{n=1}^{\infty} b_{n,\text{out}} \cdot \sin(n\omega_{rep} t) \tag{4}$$

with the Fourier coefficients

$$b_{n,\text{out}} = \hat{U} \frac{T_{BB}}{T_{rep}} \left[\text{si}\left(\pi \left[n \frac{T_{BB}}{T_{rep}} + 1 \right]\right) - \text{si}\left(\pi \left[n \frac{T_{BB}}{T_{rep}} - 1 \right]\right)\right]. \tag{5}$$

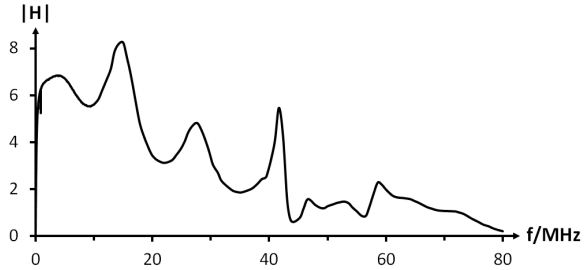

Figure 3: Measured amplitude response of the ESR BB system.

Due to linearity, the input signal for the linear region of the system can be derived from Eq. (1) and (4):

$$U_{in}(t) = \sum_{n=1}^{\infty} \frac{b_{n,\text{out}}}{|\underline{H}(n\omega_{rep})|} \cdot \sin\left(n\omega_{rep} t - \arg[\underline{H}(n\omega_{rep})]\right). \tag{6}$$

Measurements at the prototype system showed that the linear method can produce signals of sufficiently high quality up to gap voltages of about 550 V peak. A measurement of the predistorted input signal and the corresponding output signal for $f_{BB} = 5\,\text{MHz}$ and $f_{rep} = 900\,\text{kHz}$ is shown in Fig. 4.

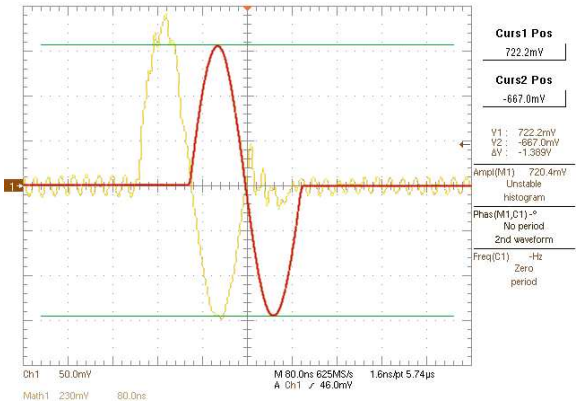

Figure 4: Measured input and output signal in the linear region ($\hat{U} = 520\,V$).

NONLINEAR APPROACH

To improve signal quality at high amplitudes, nonlinear effects have to be taken into account. As expected, measurements taken with the solid state amplifier showed that the output nonlinearly depends on the amplitude of the input signal. Therefore, the amplifier is modeled as a nonlinear voltage-controlled voltage source followed by an unknown output impedance (Fig. 2). For the cavity, only linear effects are expected that determine the dynamic behaviour, as the magnetic field strength inside the MA ring cores of the cav-

ity is far below ($\leq$ 5%) saturation field strength [16]. Presuming ideal matching between the signal generator and the amplifier input, it seems reasonable to hypothesize a Hammerstein system (a static nonlinearity followed by a linear system, e.g. [17-19]) as a simplified nonlinear model for the system (see Fig. 2).

To characterize the static nonlinearity, a power series ansatz was chosen. With an Nth-order power series, the relation between U_{in} and $U_?$ can be described as

$$U_?(t) = \sum_{n=1}^{N} a_n \left[U_{in}(t)\right]^n . \tag{7}$$

Since $U_?(t)$ can't be externally measured, $\underline{U_?}(\omega)$ was calculated in the frequency domain from the measured output voltage $U_{out}(t)$ using the frequency response measured afore:

$$\underline{U_?}(\omega) = \underline{U_{out}}(\omega) \cdot \underline{H}^{-1}(\omega). \tag{8}$$

Afterwards, $\underline{U_?}(\omega)$ is transformed back into time domain. The estimation of the coefficients a_n in Eq. (7) can be treated as a linear optimization problem by comparing single samples $U_{?,i} = U_?(i \cdot \Delta t)$ with the corresponding samples of the input signal $U_{in,i} = U_{in}(i \cdot \Delta t)$. For an input signal of M samples and a power series of order N, Eq. (7) yields

$$\begin{pmatrix} U_{in,1} & U_{in,1}^2 & \dots & U_{in,1}^N \\ U_{in,2} & U_{in,2}^2 & \dots & U_{in,2}^N \\ \vdots & \vdots & \ddots & \vdots \\ U_{in,M} & U_{in,M}^2 & \dots & U_{in,M}^N \end{pmatrix} \cdot \begin{pmatrix} a_1 \\ a_2 \\ \vdots \\ a_N \end{pmatrix} = \begin{pmatrix} U_{?,1} \\ U_{?,2} \\ \vdots \\ U_{?,M} \end{pmatrix}. \tag{9}$$

As usually $M > N$ applies, Eq. (9) is overdetermined and was solved using a least-square algorithm. Linearly predistorted signals according to Eq. (6) with different amplitudes were used for $U_{in}(t)$. Figure 5 shows a comparison of $U_{in}(t)$ and $U_?(t)$ calculated with Eq. (8).

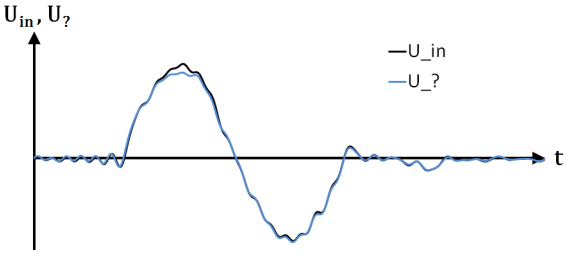

Figure 5: Comparison of U_{in} and $U_?$ for $\hat{U}_{in} = 280\ \mathrm{mV_{pp}}$.

Measurements showed that best output qualities can be achieved with power series of 3rd or 4th order. The resulting 3rd order nonlinear characteristic is shown in Fig. 6.

Based on the measured characteristic, the inverse characteristic was computed and stored in form of a look-up table. To include the nonlinear part of the model in the input signal calculation, the signal calculated for the linear region according to Eq. (6) is predistorted using the inverse characteristic of the look-up table. The resulting output signals are shown in Fig. 7.

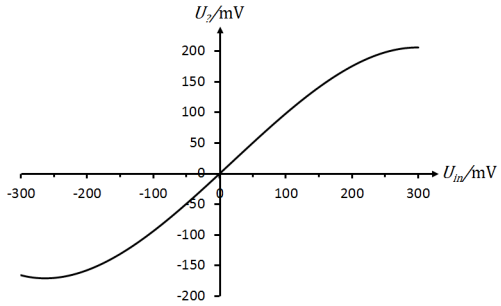

Figure 6: Measured 3rd order polynomial nonlinearity.

The additional nonlinear predistortion obviously leads to a significant improvement of the output voltage quality. Ringing can be reduced to below 1% which fulfills the specification. The difference between positive and negative half-cycle is 7% which is slightly outside the specification. However, all requirements can be satisfied when the output amplitude is reduced to 760 V. During the measurements it also became visible, that the positive half-cycle of the output voltage can't be increased much above 820 V independent of the input voltage. This might indicate that the pulse-power limit of the amplifier is reached. In that case, further increase of the amplitude for the given system is not possible.

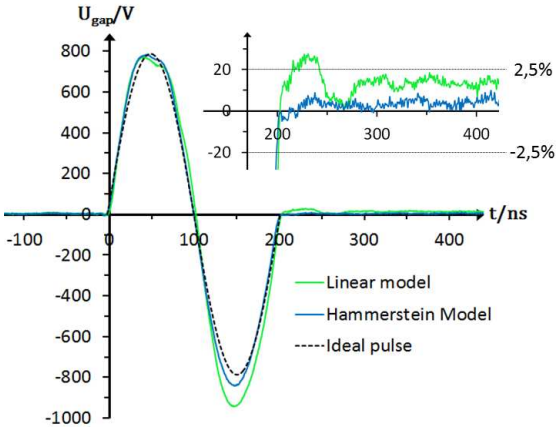

Figure 7: Resulting voltages for linear and nonlinear predistortion for $\hat{U} = 800\,V$.

CONCLUSION

Measurements at a BB prototype system showed that the current linear method is able to generate single sine gap signals of high quality in a wide voltage range. It was also shown that the assumption of a static nonlinearity in form of a 3rd order polynomial can significantly improve the gap signal quality at high amplitudes. One possibility to further increase the output quality and amplitude could be to try different parametrizations for the estimation of the nonlinear characteristic or to use a more complex model. However, measurements indicate that the amplifier of the prototype system reaches its pulse-power limit at an output amplitude of about 800 V. Therefore, a further increase of the output voltage might not be possible even with a more complex model.

REFERENCES

[1] H. H. Gutbrod *et al.*, "FAIR - Baseline Technical Report, Volume 2, Accelerator and Scientific Infrastructure", GSI, Darmstadt, Germany, September 2006.

[2] M. Steck *et al.*, "Demonstration of Longitudinal Stacking in the ESR with Barrier Buckets and Stochastic Cooling", in *Proc. COOL 2011*, Alushta, Ukraine, September 2011, paper TUPS20, pp. 140-143.

[3] C. M. Bhat, "Applications of barrier bucket RF systems at Fermilab", FNAL, Batavia IL, USA, Rep. FERMILAB-CONF-06-102-AD, March 2006.

[4] C. M. Bhat, "Particle dynamics in storage rings with barrier rf systems", *Physical Review E*, vol. 55, no. 5, p. 5992, May 1997.

[5] H. Klingbeil, U. Laier and D. Lens, "Theoretical Foundations of Synchrotron and Storage Ring RF Systems", Springer, Heidelberg, Germany, 2015.

[6] C. M. Bhat, "Barrier rf systems in synchrotrons", FNAL, Batavia IL, USA, Rep. FERMILAB-CONF-04-091-AD, 2004.

[7] O. Boine-Frankenheim, "RF barrier compression with space charge", in *Physical Review* ST Accel. Beams 13, 034202, Germany, March 2010.

[8] M. Krestnikov *et al.*, "Particle Accumulation Using Barrier Bucket RF System", in *Proc. COOL'09*, Lanzhou, China, 2009, paper TUM2MCIO02, pp. 67-70.

[9] M. Frey, D. Domont-Yankulova, J. Harzheim, K. Groß and H. Klingbeil, "Prototype Results of the ESR Barrier Bucket System", in *Proc. IPAC'17*, Copenhagen, Denmark, May 2017, paper THPIK015, this conference.

[10] K. Gross, D. Domont-Yankulova, M. Frey, J. Harzheim and H. Klingbeil, "Test Setup for Automated Barrier Bucket Signal Generation", in *Proc. IPAC'17*, Copenhagen, Denmark, May 2017, paper THPAB098, this conference.

[11] C. Ohmori *et al.*, "A wideband RF cavity for JHF synchrotrons", in *Proc. Particle Accelerator Conference 1997*, Vancouver, BC, Canada, May 1997, pp. 2995-2997.

[12] T. Trupp, "NANOPERM® Broad Band Magnetic Alloy Cores for Synchrotron RF Systems", in *Proc. IPAC'14*, Dresden, Germany, 2004, paper MOPRO016, pp. 95-98.

[13] J. Harzheim, D. Domont-Yankulova, M. Frey, H. Klingbeil and R. Königstein, "Modeling and Simulation of Broadband RF Cavities in PSpice", in *Proc. IPAC'16*, Busan, Korea, May 2016, paper MOPMW002, pp. 392–395.

[14] GSI PBRF Department, "Detailed Specification of the SIS100 Barrier Bucket System for FAIR", GSI internal report, GSI Darmstadt, Germany, August 2016.

[15] S. Jatta and K. Gross, "Spectrum of the BB signal at different periodicities", GSI internal report, GSI Darmstadt, Germany, November 2013.

[16] J. Harzheim, "Zusammenfassung nichtlineare Vorverzerrung", GSI internal report, GSI Darmstadt, Germany, December 2016.

[17] O. Nelles, "Nonlinear System Identification", Springer, Heidelberg, Germany, 2001.

[18] P. Gilabert, G. Montoro, and E. Bertran. "On the Wiener and Hammerstein models for power amplifier predistortion", in *Proc. APMC'05*, Suzhou, China, December 2005.

[19] Isaksson, Magnus, David Wisell and Daniel Ronnow. "A comparative analysis of behavioral models for RF power amplifiers", IEEE transactions on microwave theory and techniques 54.1, 2006, pp. 348-359.